

Effect of Zirconium on the Oxygen Solubility in Liquid Nickel and Ni–Fe Melts

A. A. Aleksandrov* and V. Ya. Dashevskii

Baikov Institute of Metallurgy and Materials Science, Russian Academy of Sciences,
Leninskii pr. 49, Moscow, 119334 Russia

*e-mail: a.a.aleksandrov@gmail.com

Received November 13, 2015

Abstract—The oxygen solubility in liquid nickel containing zirconium is studied experimentally for the first time at 1873 K. The equilibrium constants of the reaction of interaction between zirconium and oxygen dissolved in liquid nickel, the interaction parameters characterizing these solutions, and the zirconium activity coefficient in nickel at infinite dilution are found. The equilibrium constants of the reaction of interaction between zirconium and oxygen dissolved in the melt, the Gibbs energy of the reaction of interaction between zirconium and oxygen, and the interaction parameters characterizing these solutions are calculated at 1873 K for a wide composition range of Ni–Fe alloys. The oxygen solubility in various Ni–Fe melts containing zirconium is found at 1873 K. The deoxidizing capacity of zirconium increases as the iron content increases to 30% and decreases at higher iron content in the melt. This can be explained by the fact that an increase in the iron content lead to, on the one hand, a strengthening of the bonding forces of oxygen atoms in a melt and, on the other hand, to a significant weakening of the bonding forces of zirconium atoms with the base metal.

DOI: 10.1134/S0036029516090020

INTRODUCTION

Nickel-based alloys and Ni–Fe systems are widely used in modern engineering. Oxygen contained in these alloys reduces their operating properties. To study the physicochemical properties of the oxygen solutions in liquid nickel and Ni–Fe melts will make it possible to optimize the production of these alloys.

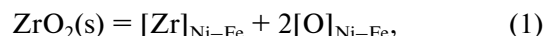
Zirconium is used as an alloying element when producing precision nickel and iron–nickel alloys. It has a higher affinity to oxygen than that of nickel or iron. If zirconium is added to an unkilld melt, its significant part can be oxidized and lost. Therefore, the study of the thermodynamics of the oxygen solutions in liquid nickel and Ni–Fe melts containing zirconium is interesting from scientific and practical points of view.

The oxygen solubility in liquid zirconium-containing liquid iron at 1873 K was studied experimentally in [1–3]. As is seen from Fig. 1, the deoxidizing capacity of zirconium in iron determined in [2] was slightly lower than that reported in [1, 3]. It should also be noted that the data in [2] demonstrated a significant scatter. The handbook [4] recommends the data from [1] as most reliable. In [1], the dependence of the oxygen solubility in liquid iron on the zirconium content was determined for four very low zirconium contents in the range 7×10^{-5} – 2×10^{-3} % Zr (Fig. 1). The range of zirconium contents studied in [3] was substantially wider (2×10^{-3} –0.65% Zr). As is seen from Fig. 1, works [1, 3] complement each other well. Although the calculation data in [5] characterize the deoxidizing

capacity of zirconium in liquid nickel, they cannot be considered as final results because of the absence of experimental data on the oxygen solubility in zirconium-containing nickel.

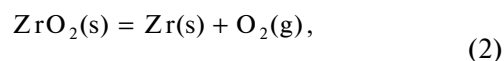
THERMODYNAMIC ANALYSIS

The product of interaction between zirconium and oxygen dissolved in Ni–Fe melts is ZrO_2 . The interaction between zirconium and oxygen dissolved in the liquid metal,

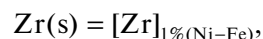


$$K_{(1)} = \frac{([\%Zr] f_{Zr}) ([\%O] f_O)^2}{a_{ZrO_2}}, \quad (1a)$$

can be represented as the sum of the reactions



$$\Delta G_{(2)}^\circ = 1081848 - 179.74T, \text{ J/mol [5]},$$



$$\Delta G_{(3)}^\circ = RT \ln \left(\frac{\gamma_{Zr(Ni-Fe)}^\circ M_{Ni-Fe}}{M_{Zr} \times 100} \right), \quad (3)$$



$$\Delta G_{(4)}^\circ = 2RT \ln \left(\frac{\gamma_{O(Ni-Fe)}^\circ M_{Ni-Fe}}{M_O \times 100} \right), \quad (4)$$

where f_i and a_i are the activity coefficient and the activity of component i , respectively; γ_i° is the activity coefficient of component i at infinite dissolution; and M_i is the molecular mass of the corresponding component.

The Gibbs energy of reaction (1) is

$$\Delta G_{(1)}^\circ = \Delta G_{(2)}^\circ + \Delta G_{(3)}^\circ + \Delta G_{(4)}^\circ.$$

The oxygen content in Ni–Fe melts in equilibrium with a given zirconium content can be calculated using the equation

$$\log[\% \text{O}]_{\text{Ni-Fe}} = \frac{1}{2} \left\{ \log K_{(1)} + \log a_{\text{ZrO}_2} - \log[\% \text{Zr}] - [e_{\text{Zr}(\text{Ni-Fe})}^{\text{Zr}} + 2e_{\text{O}(\text{Ni-Fe})}^{\text{Zr}}][\% \text{Zr}] - [2e_{\text{O}(\text{Ni-Fe})}^{\text{O}} + e_{\text{Zr}(\text{Ni-Fe})}^{\text{O}}][\% \text{O}] \right\}, \quad (5)$$

where e_i^j is the first-order interaction parameter when the component contents are expressed in wt %. At 1873 K, oxide ZrO_2 is solid ($T_m = 2993 \text{ K}$ [6]); i.e., its activity is $a_{\text{ZrO}_2} = 1$. Since quantity $[\% \text{O}]$ in the right-hand side of Eq. (5) is small, it can be expressed via the ratio $(K_{(1)}/[\% \text{Zr}])^{1/2}$ if we take $f_{\text{Zr}} \approx 1$ and $f_{\text{O}} \approx 1$ in Eq. (1a). This replacement did not give a marked error in the calculations [5]. Then, Eq. (5) takes the form

$$\log[\% \text{O}]_{\text{Ni-Fe}} = \frac{1}{2} \left\{ \log K_{(1)} - \log[\% \text{Zr}] - [e_{\text{Zr}(\text{Ni-Fe})}^{\text{Zr}} + 2e_{\text{O}(\text{Ni-Fe})}^{\text{Zr}}][\% \text{Zr}] - [2e_{\text{O}(\text{Ni-Fe})}^{\text{O}} + e_{\text{Zr}(\text{Ni-Fe})}^{\text{O}}](K_{(1)}/[\% \text{Zr}])^{1/2} \right\} \quad (5a)$$

or, in general form,

$$\log[\% \text{O}]_{\text{Ni-Fe}} = A - 1/2 \log[\% \text{Zr}] + B[\% \text{Zr}] + C/[\% \text{Zr}]^{1/2}, \quad (6)$$

where $A = 1/2 \log K_{(1)}$, $B = -1/2[e_{\text{Zr}(\text{Ni-Fe})}^{\text{Zr}} + 2e_{\text{O}(\text{Ni-Fe})}^{\text{Zr}}]$, and $C = -1/2[2e_{\text{O}(\text{Ni-Fe})}^{\text{O}} + e_{\text{Zr}(\text{Ni-Fe})}^{\text{O}}](K_{(1)})^{1/2}$.

The simultaneous processing of the experimental data from [1, 3] using Eq. (6) and regression analysis gave the following coefficients in this equation at 1873 K (coefficient of determination is $R^2 = 0.72$):

$$\log[\% \text{O}]_{\text{Fe}} = -4.179 - 1/2 \log[\% \text{Zr}] + 2.418[\% \text{Zr}] + 0.680 \times 10^{-3}/[\% \text{Zr}]^{1/2}. \quad (7)$$

The dotted curve in Fig. 1 was calculated by Eq. (7).

Taking into account the numerical values of the coefficients in Eq. (7), $e_{\text{O}(\text{Fe})}^{\text{O}} = -0.17$ [4], and the fact that $\varepsilon_{\text{Zr}}^{\text{O}} = \varepsilon_{\text{O}}^{\text{Zr}}$ [7] (ε_i^j is the first-order interaction parameter as the component concentration is expressed in mole fractions), we obtain $e_{\text{Zr}(\text{Fe})}^{\text{O}} = -20.21$, $e_{\text{O}(\text{Fe})}^{\text{Zr}} =$

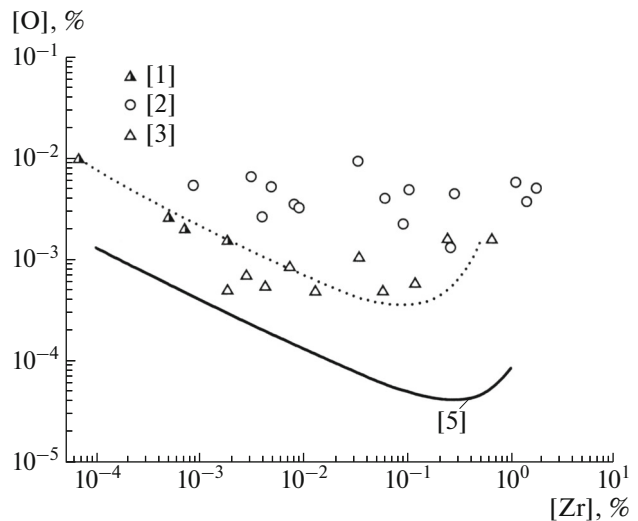


Fig. 1. Equilibrium oxygen content in pure iron and nickel [5] vs. the zirconium content at 1873 K: (points) data of [1–3] and (dotted curve) calculation by Eq. (7).

-3.54 , $e_{\text{Zr}(\text{Fe})}^{\text{Zr}} = 2.25$, $\log K_{(1)(\text{Fe})} = -8.358$, and $K_{(1)(\text{Fe})} = 4.385 \times 10^{-9}$. Then, we have $\Delta G_{(1)(\text{Fe})}^\circ = 299704 \text{ J/mol}$.

If $\Delta G_{(1)(\text{Fe})}^\circ$ is known, the Gibbs energy of reaction (3) can be found using $\Delta G_{(2)(\text{Fe})}^\circ = 745195 \text{ J/mol}$ and $\Delta G_{(4)(\text{Fe})}^\circ = -247011 \text{ J/mol}$ (the activity coefficient $\gamma_{\text{O}(\text{Fe})}^\circ = 0.0103$ [4]) calculated at 1873 K. We obtain $\Delta G_{(3)(\text{Fe})}^\circ = -198480 \text{ J/mol}$ and, then, calculate $\gamma_{\text{Zr}(\text{Fe})}^\circ$ using the equation

$$\ln \gamma_{\text{Zr}(\text{Fe})}^\circ = \frac{\Delta G_{(3)}^\circ}{RT} + \ln \left(\frac{M_{\text{Zr}} \times 100}{M_{\text{Fe}}} \right).$$

At 1873 K, we have $\gamma_{\text{Zr}(\text{Fe})}^\circ = 4.76 \times 10^{-4}$.

EXPERIMENTAL

The oxygen solubility in zirconium-containing liquid nickel was studied for the first time. Experiments were performed in an induction furnace powered by a high-frequency 10-kVA generator (400 kHz). Figure 2 shows the scheme of the experimental unit. The charge consisted of electrolytic nickel (99.95% Ni) and zirconium iodide (99.99% Zr). The charge mass was $\sim 100 \text{ g}$. A metal sample was placed in a ZrO_2 crucible, which was situated in an external Al_2O_3 crucible. The charge was loaded into a melting chamber and melted in an Ar– H_2 atmosphere. Hydrogen and argon were preliminarily passed through a system of removing oxygen, water vapor, sulfide compounds, organic

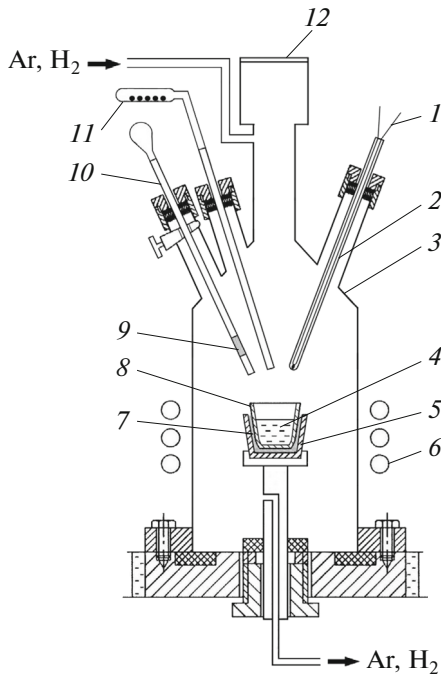


Fig. 2. Schematic diagram of the experimental unit: (1) thermocouple, (2) protecting quartz tube, (3) quartz melting chamber, (4) melt, (5) Al_2O_3 crucible, (6) inductor, (7) Al_2O_3 filling, (8) ZrO_2 crucible, (9) mold, (10) sampling device, (11) device for introducing additions, and (12) viewing window.

materials, and mechanical impurities. The argon and hydrogen flow rates were 150 mL/min and 50 mL/min, respectively. After the metal was melted, hydrogen supply was terminated and the heat was performed in an argon atmosphere (flow rate was 150 mL/min) at a temperature of 1873 K. Zirconium additions were introduced into liquid nickel without breaking the air-tightness of the furnace; then, the melt was held at this temperature to attain equilibrium in an argon atmosphere. The temperature was measured by a Pt-6% Rh/Pt-30% Rh thermocouple.

Table 1. Equilibrium contents of zirconium and oxygen in liquid nickel at 1873 K (experimental data)

[Zr], %	[O], %	[Zr], %	[O], %
0.0059	0.00579	0.61	0.00051
0.009	0.00345	0.71	0.00077
0.045	0.00248	0.98	0.00060
0.18	0.00202	1.02	0.00080
0.29	0.00062	1.26	0.00076
0.35	0.00076	1.33	0.00078
0.47	0.00060	1.39	0.00071
0.52	0.00068	1.88	0.00079

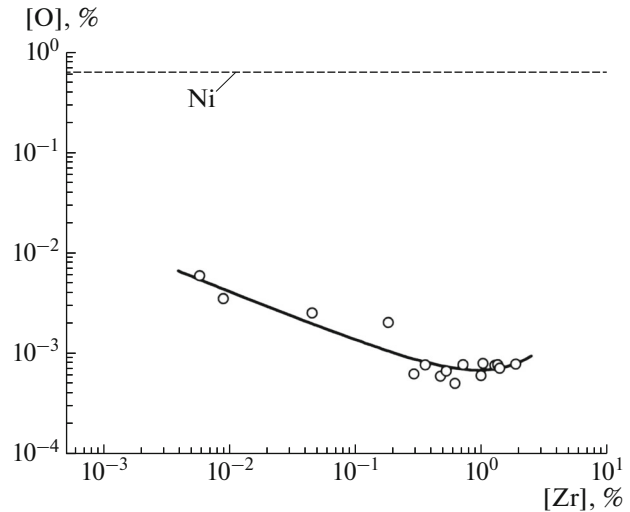


Fig. 3. Change in the oxygen content in liquid nickel as a function of the zirconium content at 1873 K: (points) experimental data and (line) calculation by Eq. (8).

During preliminary experiments, sampling was performed every 5 min, samples were analyzed to determine the zirconium and oxygen contents, and it was shown that the system attained equilibrium ~20 min after introducing a zirconium addition. In subsequent experiments, the duration of holding the melt after addition on zirconium was ~30 min to attain equilibrium reliably. Sampling was performed after the system attained equilibrium.

An analysis of metallic samples to determine the oxygen content was performed using a TC-600 (LECO) gas analyzer, and the zirconium content was determined with an ULTIMA 2 (Horiba Jobin Yvon) atomic-emission induction-plasma spectrometer.

RESULTS AND DISCUSSION

The experimental results are given in Table 1 and Fig. 3. The zirconium content in the melt was varied from 0.0059 to 1.88%. Figure 3 shows (dashed line) the oxygen solubility in pure nickel ($[\text{O}]_{\text{Ni}} = 0.636\%$ at 1873 K [8]).

The experimental data were processed by Eq. (6) using regression analysis. We obtained the following coefficients in this equation (coefficient of determination was $R^2 = 0.74$):

$$\log[\% \text{O}]_{\text{Ni}}^{\text{exp}} = -3.394 - 1/2 \log[\% \text{Zr}] + 0.227[\% \text{Zr}] + 0.405 \times 10^{-3} / [\% \text{Zr}]^{1/2}. \quad (8)$$

With allowance for the numerical values of the coefficients in Eq. (8) and the value $e_{\text{O}(\text{Ni})}^{\text{O}} = 0$ [9], we found for pure nickel at 1873 K: $e_{\text{Zr}(\text{Ni})}^{\text{O}} = -2.01$,

Table 2. Equilibrium constant of reaction (1), the activity coefficients, and the interaction parameters in Ni–Fe melts at 1873 K

Parameter	Value at Fe content (%) in the melt					
	0	20	40	60	80	100
$\Delta G_{(1)}^{\circ}$, J/mol	243406	223221	226372	244812	271381	299704
$\log K_{(1)}$	-6.788	-6.232	-6.320	-6.835	-7.577	-8.358
X_{Ni}	1.0	0.792	0.588	0.388	0.192	0
X_{Fe}	0	0.208	0.412	0.612	0.808	1.0
$M_{\text{Ni-Fe}}$	58.690	58.098	57.519	56.950	56.393	55.847
$\gamma_{\text{Zr}}^{\circ}$	1.03×10^{-8}	2.41×10^{-8}	2.00×10^{-7}	3.07×10^{-6}	4.87×10^{-5}	4.76×10^{-4}
$\gamma_{\text{O}}^{\circ}$	0.337 [9]	0.1171	0.0457	0.0214	0.0128	0.0103 [4]
e_{O}°	0 [9]	-0.037	-0.072	-0.106	-0.139	-0.17 [4]
$e_{\text{Zr}}^{\text{Zr}}$	0.24	0.68	1.09	1.49	1.88	2.25
e_{O}^{Zr}	-0.35	-1.04	-1.70	-2.34	-2.95	-3.54
e_{Zr}°	-2.01	-5.95	-9.73	-13.37	-16.86	-20.21

$e_{\text{O(Ni)}}^{\text{Zr}} = -0.35$, $e_{\text{Zr(Ni)}}^{\text{Zr}} = 0.24$, $\log K_{(1)(\text{Ni})} = -6.788$,
 $K_{(1)(\text{Ni})} = 1.629 \times 10^{-7}$, and $\Delta G_{(1)(\text{Ni})}^{\circ} = 243406$ J/mol.

If $\Delta G_{(1)(\text{Ni})}^{\circ}$ is known, the Gibbs energy of reaction (3) can be found by calculating $\Delta G_{(2)(\text{Ni})}^{\circ} = 745195$ J/mol and $\Delta G_{(4)(\text{Ni})}^{\circ} = -136829$ J/mol ($\gamma_{\text{O(Ni)}}^{\circ} = 0.337$ [9]) at 1873 K. We obtain $\Delta G_{(3)(\text{Ni})}^{\circ} = -364960$ J/mol and, then, calculate $\gamma_{\text{(Zr)(Ni)}}^{\circ}$ using the equation

$$\ln \gamma_{\text{Zr(Ni)}}^{\circ} = \frac{\Delta G_{(3)}^{\circ}}{RT} + \ln \left(\frac{M_{\text{Zr}} \times 100}{M_{\text{Ni}}} \right).$$

At 1873 K, we have $\gamma_{\text{Zr(Ni)}}^{\circ} = 1.03 \times 10^{-8}$.

Using the obtained thermodynamic parameters for pure iron and nickel, we can determine the activity coefficients and the interaction parameters of Ni–Fe alloys of various compositions (Table 2).

The molecular masses of the Ni–Fe melts were calculated by the equation [8]

$$M_{\text{Ni-Fe}} = M_{\text{Ni}} X_{\text{Ni}} + M_{\text{Fe}} X_{\text{Fe}},$$

and activity coefficient $\gamma_{i(\text{Ni-Fe})}^{\circ}$ was calculated by the formula [10]

$$\begin{aligned} \ln \gamma_{i(\text{Ni-Fe})}^{\circ} &= X_{\text{Ni}} \ln \gamma_{i(\text{Ni})}^{\circ} + X_{\text{Fe}} \ln \gamma_{i(\text{Fe})}^{\circ} \\ &+ X_{\text{Ni}} X_{\text{Fe}} \left[X_{\text{Ni}} (\ln \gamma_{i(\text{Ni})}^{\circ} - \ln \gamma_{i(\text{Fe})}^{\circ}) + \epsilon_{i(\text{Ni})}^{\text{Fe}} \right] \\ &+ X_{\text{Fe}} (\ln \gamma_{i(\text{Fe})}^{\circ} - \ln \gamma_{i(\text{Ni})}^{\circ}) + \epsilon_{i(\text{Ni})}^{\text{Ni}} \end{aligned}$$

The calculations were carried out using the following interaction parameters: $\epsilon_{\text{Zr(Fe)}}^{\text{Ni}} = -9.88$ [11], $\epsilon_{\text{O(Fe)}}^{\text{Ni}} = 0.27$ [12], and $\epsilon_{\text{O(Ni)}}^{\text{Fe}} = -5.179$ [12]. Handbooks do not have interaction parameter $\epsilon_{\text{Zr(Ni)}}^{\text{Fe}}$, and it was taken to be -0.1 by analogy with aluminum ($\epsilon_{\text{Al(Fe)}}^{\text{Ni}} = -9.143$, $\epsilon_{\text{Al(Ni)}}^{\text{Fe}} = -0.147$ [13]).

Ni–Fe melts are characterized by insignificant deviations from ideal behavior [14], which makes it possible to calculate interaction parameters $\epsilon_{i(\text{Ni-Fe})}^j$ and, correspondingly $e_{i(\text{Ni-Fe})}^j$ using, as a first approximation, the relationship [8]

$$\epsilon_{i(\text{Ni-Fe})}^j = \epsilon_{i(\text{Ni})}^j X_{\text{Ni}} + \epsilon_{i(\text{Fe})}^j X_{\text{Fe}}.$$

Table 2 gives the calculated values of Gibbs energy $\Delta G_{(1)}^{\circ}$ of reaction (1) and the equilibrium constants of this reaction ($K_{(1)}$) for various Ni–Fe alloys. Figure 4

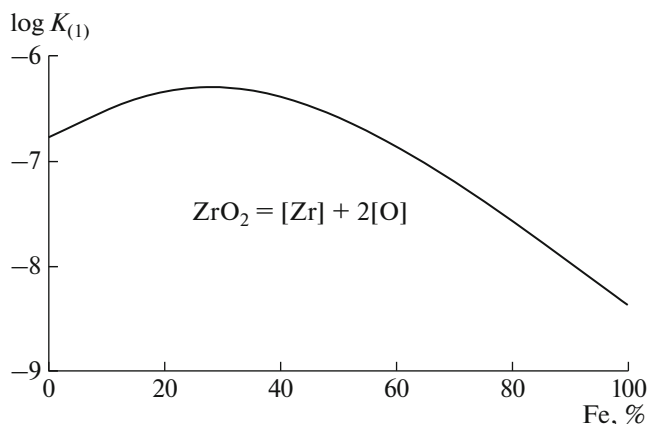


Fig. 4. Equilibrium constant of reaction (1) vs. the melt base composition at 1873 K.

shows the dependence of the equilibrium constants of reaction (1) on the composition of the base metal of the melts. It is seen that the equilibrium constant of reaction (1) increases as the iron content in the melt increases to ~30% and, then, it substantially decreases. This finding can be explained by an increase in the bonding forces between oxygen atoms with the iron content in the melt ($\gamma_{O(Ni)}^{\circ} = 0.337$; $\gamma_{O(Fe)}^{\circ} = 0.0103$) and a simultaneous significant weakening of the bonding forces between zirconium atoms and base metal atoms ($\gamma_{O(Ni)}^{\circ} = 1.03 \times 10^{-8}$, $\gamma_{Zr(Fe)}^{\circ} = 4.76 \times 10^{-4}$).

With allowance for the obtained values of the equilibrium constant of reaction (1) and the interaction parameters (Table 2), Eq. (5a) for the alloys with various compositions at 1873 takes the form

$$\log[\% O]_{Ni-20\% Fe} = -3.116 - 1/2 \log[\% Zr] + 0.703[\% Zr] + 2.306 \times 10^{-3} / [\% Zr]^{1/2}, \quad (5b)$$

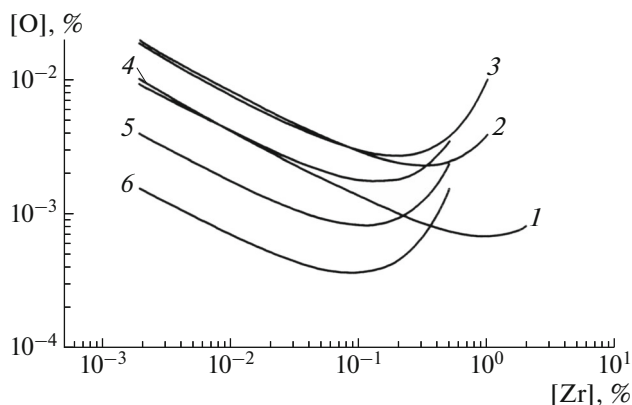


Fig. 5. Oxygen content in Ni-Fe melts as a function of the zirconium and iron contents at 1873 K ((1) 0, (2) 20, (3) 40, (4) 60, (5) 80, (6) 100% Fe).

$$\log[\% O]_{Ni-40\% Fe} = -3.160 - 1/2 \log[\% Zr] + 1.157[\% Zr] + 3.417 \times 10^{-3} / [\% Zr]^{1/2}, \quad (5c)$$

$$\log[\% O]_{Ni-60\% Fe} = -3.417 - 1/2 \log[\% Zr] + 1.594[\% Zr] + 2.597 \times 10^{-3} / [\% Zr]^{1/2}, \quad (5d)$$

$$\log[\% O]_{Ni-80\% Fe} = -3.788 - 1/2 \log[\% Zr] + 2.013[\% Zr] + 1.395 \times 10^{-3} / [\% Zr]^{1/2}. \quad (5e)$$

The dependences of the equilibrium oxygen concentration on the zirconium content in Ni-Fe melts calculated by Eqs. (5b)–(5e), (7) and (8) are presented in Table 3 and Fig. 5. According to the data obtained, the zirconium deoxidizing capacity increased as the iron content increased to 20–40% and it decreased with further increasing the iron content in melt. The Ni–20% Fe alloy had the zirconium deoxidizing capacity that is almost the same as that in the Ni–40% Fe alloy. The solubility curves of the oxygen solubility in Ni-Fe melts passed through a minimum, whose position shifted to lower zirconium contents with increasing iron content.

The oxygen solubility in zirconium-containing Ni–60% Fe alloys at 1873 K was studied in [15], and the following equation was derived for the dependence of the oxygen content on the zirconium content in the melt:

$$\log[\% O]_{Ni-60\% Fe} = -3.111 - 1/2 \log[\% Zr] + 0.172[\% Zr] + 2.856 \times 10^{-3} / [\% Zr]^{1/2}. \quad (9)$$

Moreover, the following interaction parameters were calculated: $e_{Zr(Ni-60\% Fe)}^O = -7.16$, $e_{O(Ni-60\% Fe)}^{Zr} = -1.25$, and $e_{Zr(Ni-60\% Fe)}^{Zr} = 2.16$. These data and the data of this work are compared in Fig. 6. The agreement between these results is satisfactory.

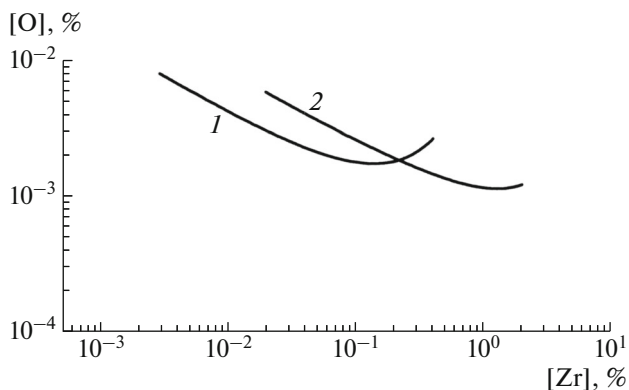


Fig. 6. Oxygen content in the Ni–60% Fe melt at 1873 K vs. the zirconium content: (1), (2) calculations by Eq. (5d) and Eq. (9), respectively.

Table 3. Equilibrium contents of zirconium and oxygen in Ni–Fe melts at 1873 K (experimental data)

[Zr], %	[O], %					
	Ni	Ni–20% Fe	Ni–40% Fe	Ni–60% Fe	Ni–80% Fe	Fe
0.001	0.01315	0.02868	0.02813	0.01466	0.00573	0.00221
0.002	0.00923	0.01934	0.01854	0.00985	0.00395	0.00155
0.005	0.00580	0.01177	0.01108	0.00599	0.00247	0.00098
0.01	0.00410	0.00820	0.00769	0.00421	0.00176	0.00071
0.02	0.00290	0.00581	0.00545	0.00304	0.00129	0.00053
0.05	0.00186	0.00380	0.00366	0.00211	0.00093	0.00039
0.1	0.00135	0.00289	0.00293	0.00178	0.00083	0.00037
0.2	0.00101	0.00239	0.00268	0.00181	0.00093	0.00045
0.5	0.00075	0.00245	0.00375	0.00342	0.00235	0.00151
1.0	0.00069	0.00388	0.01001	0.01509	0.01681	0.01725

The zirconium contents to which the minimum oxygen contents correspond can be found by the equation [16]

$$[\% R]' = -\frac{m}{2.3(me_R^R + ne_O^R)}, \quad (10)$$

where m and n are the stoichiometric coefficients in the oxide formula R_mO_n . In the case of oxide ZrO_2 , Eq. (10) takes the form

$$[\% Zr]' = -\frac{1}{2.3(e_{Zr}^{Zr} + 2e_O^{Zr})}. \quad (10a)$$

The zirconium contents at the points of minima calculated by Eq. (10a) and the corresponding oxygen contents are as follows:

Fe, %	0	20	40
[% Zr]'	0.945	0.309	0.188
[% O] _{min}	0.00069	0.00229	0.00268

Fe, %	60	80	100
[% Zr]'	0.136	0.108	0.090
[% O] _{min}	0.00174	0.00083	0.00037

CONCLUSIONS

(1) The oxygen solubility at 1873 K in liquid zirconium-containing nickel was studied for the first time. We found the equilibrium constant of the reaction of interaction between zirconium and oxygen dissolved in liquid nickel ($\log K_{(1)(Ni)} = -6.788$), the interaction parameters characterizing these solutions ($e_{Zr(Ni)}^O = -2.01$, $e_{O(Ni)}^{Zr} = -0.35$, $e_{Zr(Ni)}^{Zr} = 0.24$), and the zirconium activity coefficient at infinite dilution ($\gamma_{Zr(Ni)}^O = 1.03 \times 10^{-8}$).

(2) The Gibbs energy of the reaction of interaction between zirconium and oxygen dissolved in the melts under study, the equilibrium constant of this reaction, and the interaction parameters characterizing these solutions were calculated over a wide Ni–Fe alloy composition range. We determined the oxygen solubility at 1873 K in various zirconium-containing Ni–Fe melts.

(3) It was noted that the zirconium deoxidizing capacity increased as the iron content increased to 30% and decreased with a further increase in the iron content. This finding is explained by the fact that an increase in the iron content leads to an increase in the bonding forces between oxygen atoms in a melt ($\gamma_{O(Ni)}^O = 0.337$; $\gamma_{O(Fe)}^O = 0.0103$) and to a simultaneous significant weakening of the bonding forces between zirconium atoms and base metal atoms ($\gamma_{Zr(Ni)}^O = 1.03 \times 10^{-8}$, $\gamma_{Zr(Fe)}^O = 4.76 \times 10^{-4}$).

(4) The curves of the oxygen solubility in Ni–Fe melts were shown to pass through a minimum, the position of which shifted to low zirconium contents as the iron content increased.

ACKNOWLEDGMENTS

This work was supported by the Russian Foundation for Basic Research, project no. 14-03-31682 mol_a.

REFERENCES

- O. Kitamura, S. Ban-Ya, and T. Fuwa, "Deoxidation of liquid iron with zirconium," in *The Second Japan–USSR Joint Symposium on Physical Chemistry of Metallurgical Processes* (Iron Steel Inst. Jap., 1969), Vol. 10, pp. 47–53.
- D. Janke and W. A. Fischer, "Desoxidationsgleichgewichte von titan, aluminium und zirconium in eisen-

- schmelzen bei 1600°C,” Arch. Eisenhüttenwes **B 47** (4), 195–198 (1976).
3. R. Inoue, T. Ariyama, and H. Suito, “Thermodynamics of zirconium deoxidation equilibrium in liquid iron by EMF measurements,” ISIJ Intern. **48** (9), 1175–1181 (2008).
 4. *Steelmaking Data Sourcebook: A Handbook* (Gordon & Breach Sci. Publ., New York, 1988).
 5. I. S. Kulikov, *Deoxidation of Metals* (Metallurgiya, Moscow, 1975).
 6. *Slag Atlas* (Verlag Stahleisen GmbH, Düsseldorf, 1995).
 7. C. Wagner, *Thermodynamics of Alloys* (Metallurgizdat, Moscow, 1957).
 8. V. Ya. Dashevskii, A. A. Aleksandrov, and L. I. Leont’ev, “The thermodynamics of oxygen solutions in Fe–Ni, Fe–Co, and Co–Ni melts,” Izv. Vyschikh Ucheb. Zaved., Chern. Met., No. 1, 54–60 (2015).
 9. G. K. Sigworth, J. F. Elliott, G. Vaughn, and G. H. Geiger, “The thermodynamics of dilute liquid nickel alloys,” Met. Soc. CIM, Ann. **V**, 104–110 (1977).
 10. M. G. Froberg and M. Wang, “Thermodynamic properties of sulphur in liquid copper–antimony alloys at 1473 K,” Z. Metallkd. **B 81** (7), 513–518 (1990).
 11. Yu. P. Snitko, Yu. N. Surovoi, and N. P. Lyakishev, “Relation between the interaction parameters and the atomic characteristics of components,” Dokl. Akad. Nauk SSSR **286** (5), 1154–1156 (1983).
 12. T. Chiang and Y. A. Chang, “The activity coefficient of oxygen in binary liquid metal alloys,” Met. Trans. **B 7**, 453–457 (1976).
 13. F. Ishii, S. Ban-Ya, and M. Hino, “Thermodynamics of the deoxidation equilibrium of aluminum in liquid nickel and nickel–iron alloys,” ISIJ Intern. **36** (1), 25–31 (1996).
 14. R. Hultgren, P. D. Desai, D. T. Hawkins, et al., *Selected Values of the Thermodynamic Properties of Binary Alloys* (Metals Park, Amer. Soc. Metals, Ohio, 1973).
 15. V. Ya. Dashevskii, A. A. Aleksandrov, A. G. Kanevskii, and L. I. Leont’ev, “Oxygen solubility in zirconium-containing iron–nickel melts,” Perspektivnye Mater., No. 2, 5–10 (2014).
 16. V. Ya. Dashevskii, A. A. Aleksandrov, and L. I. Leont’ev, “Thermodynamics of the oxygen solutions upon complex deoxidizing Fe–Co melts,” Izv. Vyschikh. Ucheb. Zaved., Chern. Met., No. 5, 33–41 (2014).

Translated by Yu. Ryzhkov